

## Durham Research Online

---

### Deposited in DRO:

08 December 2010

### Version of attached file:

Published Version

### Peer-review status of attached file:

Peer-reviewed

### Citation for published item:

Kaliteevski, M.A. and Beggs, D.M. and Brand, S. and Abram, R.A. and Nikolaev, V.V. (2006) 'Statistics of the eigenmodes and optical properties of one-dimensional disordered photonic crystals.', *Physical review E*, 73 (5). 056616.

### Further information on publisher's website:

<http://dx.doi.org/10.1103/PhysRevE.73.056616>

### Publisher's copyright statement:

© 2006 by The American Physical Society. All rights reserved.

### Additional information:

---

## Use policy

The full-text may be used and/or reproduced, and given to third parties in any format or medium, without prior permission or charge, for personal research or study, educational, or not-for-profit purposes provided that:

- a full bibliographic reference is made to the original source
- a [link](#) is made to the metadata record in DRO
- the full-text is not changed in any way

The full-text must not be sold in any format or medium without the formal permission of the copyright holders.

Please consult the [full DRO policy](#) for further details.

# Statistics of the eigenmodes and optical properties of one-dimensional disordered photonic crystals

M. A. Kaliteevski,\* D. M. Beggs, S. Brand, and R. A. Abram

*Department of Physics, University of Durham, Durham, DH1 3LE, United Kingdom*

V. V. Nikolaev

*Ioffe Physicotechnical Institute, 26, Polytechnicheskaya, St. Petersburg, Russia*

(Received 22 December 2005; published 31 May 2006)

The eigenmode spectrum and transmission properties of a certain class of one-dimensional disordered photonic crystals have been studied statistically. It is shown that the relative fluctuation of the optical width of the period of the photonic crystal is a universal parameter allowing a quantitative description of the disordered photonic crystal for various models of disorder. It is shown that the tail of the density of states is characterized by a certain penetration depth and a quantitative relation between the penetration depth, the relative band gap width, and the disorder parameter is obtained. It is found that a threshold level of disorder exists, below which the density of states in the center of the photonic band gap vanishes, and the ensemble-averaged transmission coefficient does not change significantly with increasing disorder. Also, the standard deviation of the transmission coefficient is less than its mean value. Above threshold, the ensemble averaged transmission coefficient and density of states increase with the level of disorder rapidly, and the standard deviation of the transmission coefficient exceeds its mean value. A scaling formula is presented, which relates the logarithm of the transmission to the periodic refractive index modulation and the disorder.

DOI: [10.1103/PhysRevE.73.056616](https://doi.org/10.1103/PhysRevE.73.056616)

PACS number(s): 42.70.Qs, 79.60.Ht

## I. INTRODUCTION

Interest in the properties of disordered photonic crystals [1,2] has arisen for various reasons, including the necessity to produce photonic crystals for technical applications, whose photonic band gap (PBG) will not be significantly degraded (filled with photonic states) due to disorder, and also because of the possibility of light localization in such structures [3]. Despite the continual enhancement in the technology of photonic crystal fabrication, samples are inevitably disordered to a greater or lesser extent. For example, in self-organized photonic crystals, such as opals, the size of the spheres tends to vary, and photonic crystals produced by lithography are not ideal due to the roughness of the walls and the nonuniformity in the depth of the etched elements.

It has been known for a long time that disorder in semiconductors can lead to the localization of carriers, which is manifested in a decrease of electric conductivity [4,5]. For example, the impurity band of a lightly doped, nearly compensated *n*-type semiconductor at low temperature is disordered due to the random locations of the impurities and is occupied by electrons at a density small compared to that of the impurity centers because of the compensation. In such a system, the relatively low density of electrons means that electron-electron interactions can be neglected and the low temperature results in a low level of phonon scattering, and localization of electrons due to disorder can be observed.

Although not directly applicable to the semiconductor impurity band, the Anderson model provides an elegant picture

of how electron localization can occur in a disordered electronic system. According to the one-dimensional Anderson model, an electron placed in a sequence of quantum wells is localized even for a small disorder. In mathematical language the latter means that even for small fluctuations of the energy levels of the individual quantum wells in an infinite one-dimensional system, the wave function of the electron decays exponentially with distance from a certain bounded domain in space.

More recently it has been proposed, that a related phenomenon—localization of photons—can be observed in disordered dielectric structures [6]. To describe photon localization it initially seemed natural to use analogies with the theory of electrons in solids, since the electromagnetic field and the quantum mechanics of electrons are both governed by wave equations and the theory of electron localization was already well developed [7,8] and provided a good description of experimentally observed phenomena.

However, there are important differences between the wave equation for the electric field of light of angular frequency  $\omega$ ,

$$\vec{\nabla} \times \vec{\nabla} \times \mathbf{E}(\mathbf{r}) = \varepsilon(\mathbf{r}) \frac{\omega^2}{c^2} \mathbf{E}(\mathbf{r}) \quad (1)$$

or

$$\vec{\nabla} \times \vec{\nabla} \times \mathbf{E}(\mathbf{r}) + [\varepsilon(\mathbf{r}) - 1] \frac{\omega^2}{c^2} \mathbf{E}(\mathbf{r}) = \frac{\omega^2}{c^2} \mathbf{E}(\mathbf{r}) \quad (2)$$

spatial dependence of the dielectric constant  $\varepsilon(\mathbf{r}) = \varepsilon_{\text{per}}(\mathbf{r}) + \varepsilon_{\text{fluct}}(\mathbf{r})$  includes periodic  $\varepsilon_{\text{per}}(\mathbf{r})$  and random parts  $\varepsilon_{\text{fluct}}(\mathbf{r})$ , and the Schrödinger equation for electrons of energy  $U$

\*Corresponding author. Email address: [mikhail.kaliteevski@durham.ac.uk](mailto:mikhail.kaliteevski@durham.ac.uk)

$$-\frac{\hbar^2}{2m}\nabla^2\psi + V(\mathbf{r})\psi = U\psi, \quad (3)$$

where the potential  $V(\mathbf{r}) = V_{\text{per}}(\mathbf{r}) + V_{\text{fluct}}(\mathbf{r})$  has analogous components. The potential  $V(\mathbf{r})$  can be positive or negative, and  $V(\mathbf{r})$  in (3) is independent of  $U$ . In contrast, the dielectric constant  $\epsilon(\mathbf{r})$  in nonabsorbing media has a real positive value and enters in (1) as a product with  $\omega^2$ . It follows that for an electron of energy  $U$ , a potential can exist where in the local surrounding region  $V(\mathbf{r}) > U$ . Furthermore, states with values of an energy less than the mean potential of the system can occur. For photons the analogous situation is not possible. In particular, the Anderson model is not a suitable analog of a disordered photonic system since it starts from the existence of localized electron states in individual quantum wells. Nevertheless, coherent backscattering (weak localization of photons) [9–11], which is assumed to be a precursor of “real localization,” has been observed experimentally, which supports the hypothesis that light localization in dielectric disordered structures is possible.

From the fundamental point of view another important difference between disordered photonic and electronic systems is that the former are in many ways easier to study experimentally. The behavior of the electrical conductivity can be used to detect and probe electron localization but the effects of the phenomenon in many systems are obscured by the electron-electron interaction, phonon scattering, the contacts, and the fact that the current measured is usually the resultant effect of many electrons. In contrast, photon-photon scattering does not occur in linear optical media and scattering by phonons is negligible. Further, the coherence of the photonic states is conserved across a typical photonic microstructure and it is possible to detect photons in a single or small number of modes. However, optical measurements on photonic structures do raise the question of what is meant by a localized state in a finite system, and also how do we know when we have observed one [12]. For example transmission experiments can produce what at first sight are counterintuitive results, such as near 100% transmission, independent of sample length, that occur at frequencies close to localized photonic states.

Localization of photons can be achieved in microcavities [13], which are isolated defects (for example, a half-wave layer) in a photonic crystal (such as a Bragg reflector, which is a periodic sequence of pairs of quarter-wave layers), where the density of electromagnetic energy of an eigenmode  $\eta$  decays with position  $z$  relative to the microcavity as

$$\eta(z) \propto \exp(-|z|/\xi), \quad (4)$$

where  $\xi$  is an attenuation length. As noted above, such a localized state manifests itself as a sharp peak in the transmission spectrum irrespective of sample thickness. On the other hand, the exponential decay of light transmission with sample thickness does occur when the frequency coincides with the band gap of a photonic crystal, where there are in fact no states. Electrons exhibit analogous effects in semiconductor superlattices, as long as extraneous scattering can be avoided, but experimental observation is much more difficult. Obviously it is useful to carry out theoretical interpre-

tation of the results of light transmission (and reflection) experiments and this can be done using standard electromagnetic theory [6,14–18]. However, it is also valuable to consider more directly the properties of the states of a photonic microstructure in a way which is dependent on the properties of the system rather than any external stimulus. This can be done by considering the states that exist when outgoing wave boundary conditions are applied. In this way we can directly calculate the lifetimes of the states as well as their energies and electromagnetic field profiles. Further, the outgoing wave boundary conditions provide in principle an appropriate description of truly localized states in an infinite system, including their finite lifetime and the decaying profile of the electromagnetic field.

Experimental studies of light transmission in photonic crystals have shown, that there is a dip in the transmission spectrum within the PBG. At the frequency of the dip, light decays exponentially with distance and, hence, the transmission decreases with increasing sample thickness, but the effective attenuation length measured experimentally is generally larger than it should be for an ideal (nondisordered) structure [19–23]. However, it has been shown theoretically for a one-dimensional disordered photonic crystal [24] that, if the level of disorder does not exceed a certain threshold value, a significant increase of the attenuation length with increase of disorder does not occur. Similar results have also been obtained more recently for the two-dimensional case [25,26]. On the basis of these results, a hypothesis was proposed that the PBG is filled by localized states only when the disorder is above a certain threshold.

The aim of the present work is further investigation of the spectrum of optical eigenmodes in a one-dimensional disordered photonic crystal in the frequency region corresponding to the PBG, and the establishment of a relationship between the transmission properties and the associated modifications to the eigenmode spectrum.

## II. RESULTS AND DISCUSSION

Consider the one-dimensional infinite periodic structure, shown in Fig. 1(a), which is a sequence of pairs of layers  $A$  and  $B$  of the same thicknesses  $D/2$ , whose refractive indices are

$$n_{A,B}^{(0)} = n_0 \pm g, \quad (5)$$

where  $g$  is the modulation of the refractive index and  $n_0$  is the average refractive index. We have modeled a series of structures with  $n_0 = 1.0, 2.0, 3.0$ , and  $4.0$  and  $g = 0.0125, 0.025, 0.05, 0.75$ , and  $0.1$ .

Using a transfer matrix method, we can obtain the dispersion equation for photons in such a structure which is of the form

$$\begin{aligned} \cos(KD) = & \cos\left(\frac{n_A D \omega}{2c}\right) \cos\left(\frac{n_B D \omega}{2c}\right) - \frac{1}{2} \left(\frac{n_A}{n_B} - \frac{n_B}{n_A}\right) \\ & \times \sin\left(\frac{n_A D \omega}{2c}\right) \sin\left(\frac{n_B D \omega}{2c}\right), \end{aligned} \quad (6)$$

where  $D$  is the period of the structure and  $K$  is the Bloch

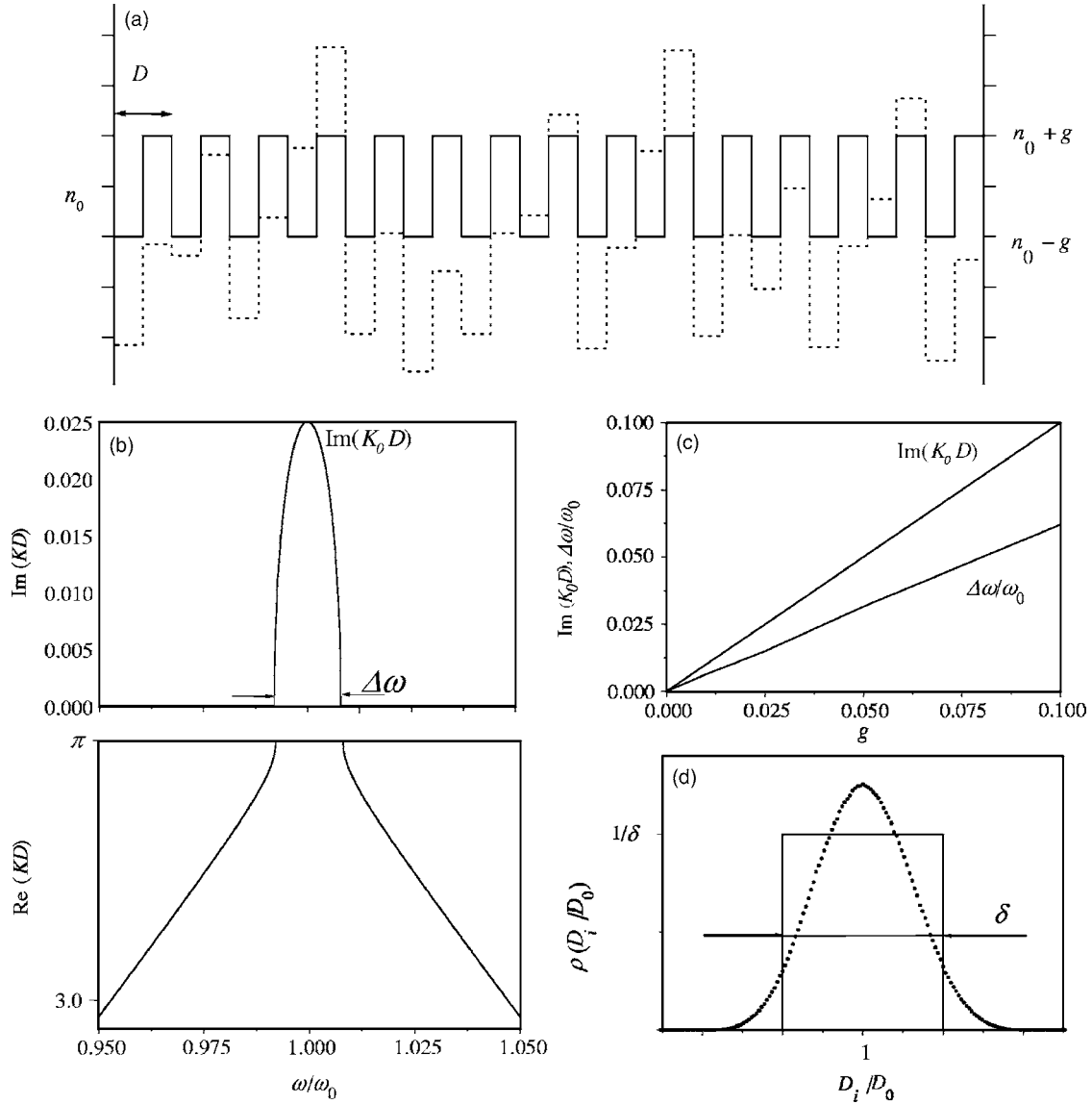


FIG. 1. (a) Profiles of the refractive indices in the ideal (solid line) and the disordered (dashed line) structures. (b) Dependence of the Bloch wave vector  $K$  on frequency  $\omega$  for the ideal structure with  $g=0.025$ . (c) Dependence of the relative PBG width  $\Delta\omega/\omega_0$  and the attenuation of light per period of the structure  $\text{Im}(K_0 D)$  at the center of the PBG as a function of the modulation of the refractive index  $g$ . (d) Distribution of the probability density of the optical lengths  $D_i$  of the period for a disordered structure. Solid line shows the distribution for fluctuations of either the refractive index or thicknesses of the layers of the unit cell according to Eqs. (8) and (9); dotted line shows the near Gaussian distribution of  $D_i$  obtained by simultaneous and independent fluctuations of layer thicknesses and refractive index characterized by a top-hat distribution of relative width  $\delta$ .

wave vector. Solving this equation one can show that there are PBGs in the mode spectrum, and the center of the first PBG is at  $\omega_0 = \pi c / (n_0 D)$ , as shown in Fig. 1(b). The relative width of the gap is  $\Delta\omega/\omega_0 \approx 4g/(\pi n_0)$ , and the attenuation of light per period is given by  $\text{Im}(K_0 D) = D/2\xi_0 = \ln|n_1/n_2| \approx 2g/n_0$  (where  $K_0$  is the imaginary part of the Bloch wave vector at frequency  $\omega_0$ , and  $\xi_0$  is the attenuation length of light at the center of PBG) and is proportional to the modulation of the refractive index  $g$ , as shown in Fig. 1(c). Note, that for the chosen value of  $n_0=2.0$ , the attenuation of light per period,  $\text{Im}(K_0) \approx g$ .

For a structure of finite size one can set outgoing wave boundary conditions, corresponding to light not being incident on the structure, and using the equation

$$\mathcal{A} \begin{pmatrix} 1 \\ -n_f \end{pmatrix} = \hat{\mathbf{M}} \begin{pmatrix} 1 \\ n_l \end{pmatrix} \quad (7)$$

obtain a spectrum of the optical eigenmodes of the structure. Here  $n_f$  and  $n_l$  are the refractive indices of the semi-infinite media surrounding the structure,  $\hat{\mathbf{M}}$  is the transfer matrix through the whole structure, and  $\mathcal{A}$  is a constant. For a structure of finite size, the eigenmode spectrum will be discrete [as shown in Fig. 2(a)], and the frequencies of the eigenmodes  $\omega_i$  will have nonzero imaginary parts, due to the leakage of the light through the boundaries. In other words, the lifetime of the eigenmodes  $\tau = 1/\text{Im}(\omega_i)$  will be finite. By analyzing the value of the lifetime, one can conclude,

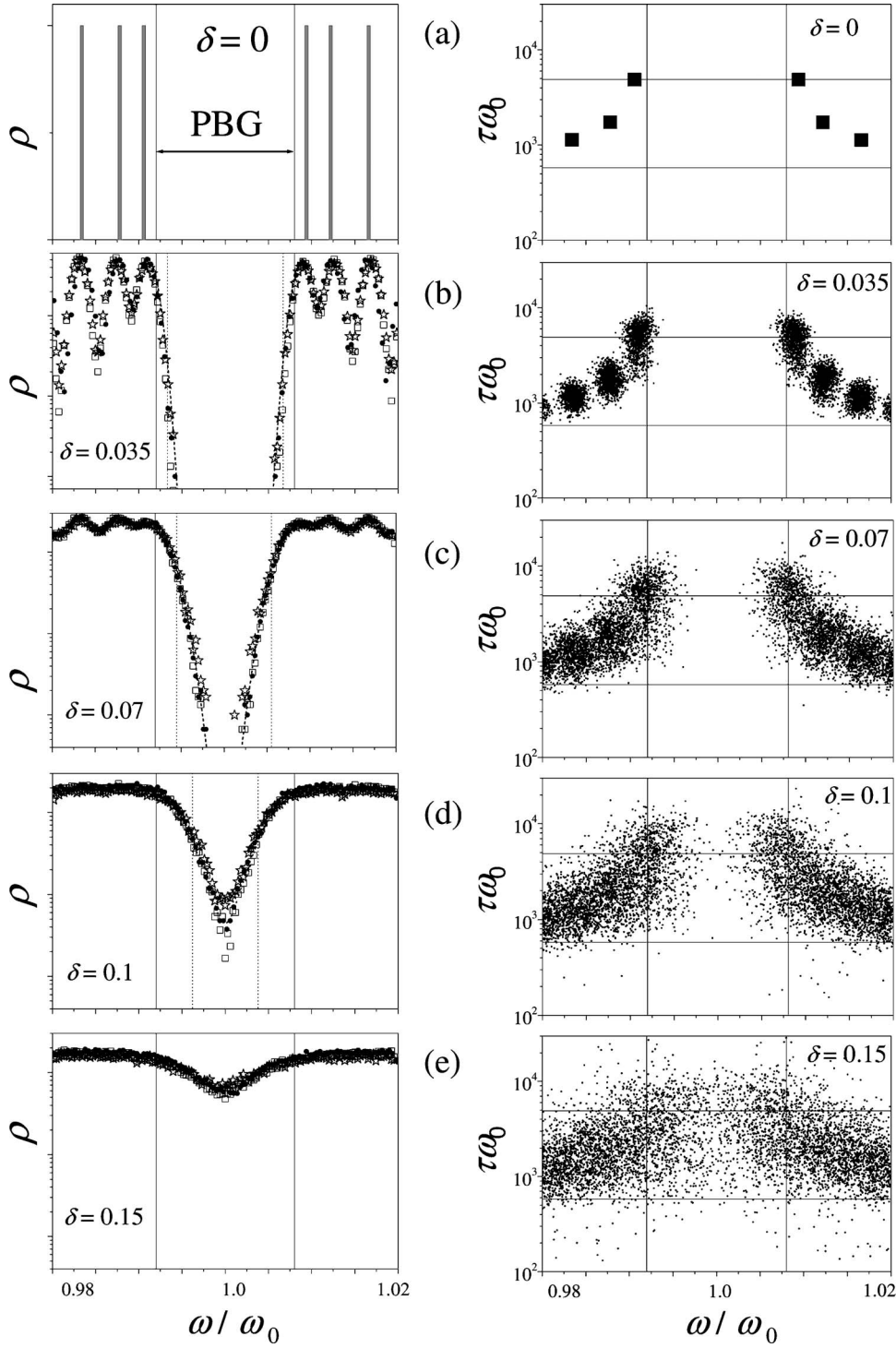


FIG. 2. (a) On the left: density of states for an ideal structure. On the right: frequencies  $\text{Re}(\omega_i)$  and lifetimes  $\tau=1/\text{Im}(\omega_i)$  for an ideal structure ( $\delta=0$ ). (b)–(e) On the left: density of states averaged over ensembles of  $10^4$  structures with  $\delta=0.035$  (b) 0.07 (c) 0.1 (d) and 0.15 (e) plotted on a logarithmic scale. On the right: frequencies  $\text{Re}(\omega_i)$  and lifetimes  $\tau=1/\text{Im}(\omega_i)$  for eigenmodes, obtained by solving Eq. (7) for  $10^3$  disordered structures. The total thickness of the structure is  $L=200D$ , and the modulation of the refractive index is  $g=0.025$ . The vertical solid lines show the boundaries of the PBG for the ideal structure. The dashed lines show the fit to the density of states within the PBG using formula (11). The vertical dotted lines indicate the penetration depth  $\Omega$  for each case. Circles (squares) correspond to fluctuations of the optical length of the periods with the square distribution in Fig. 1(d), due to fluctuations of the refractive indices (widths) of the layers. Stars correspond to the near-Gaussian distribution of  $D_i$  shown in Fig. 1(d).

whether the mode is localized or not, according to the Thouless [8] criterion. For electrons the Thouless criterion considers a state to be localized if the width of the energy level (proportional to the inverse lifetime) is less than the separation of energy levels; otherwise the state is extended.

In the transmission spectrum of an ideal periodic structure of the type shown in Fig. 1(a) there is a pronounced dip, corresponding to the PBG, and at the center of the PBG the transmission coefficient falls to  $2 \times 10^{-4}$  for a structure with  $n_0=2.0$ ,  $g=0.025$ , and thickness  $L=200D$  surrounded by

semi-infinite media with refractive index equal to unity, as shown in Fig. 3.

For the study of the properties of disordered structures we introduce random fluctuations of the refractive indices: for each pair of layers  $A$  and  $B$  in the unit cell, the refractive indices are defined by the formula

$$n_{A,B} = n_0 \pm g + n_0 \delta P, \quad (8)$$

where  $P$  takes random values in the interval from  $-1/2$  to  $1/2$  and  $\delta$  is the constant for a particular structure that speci-



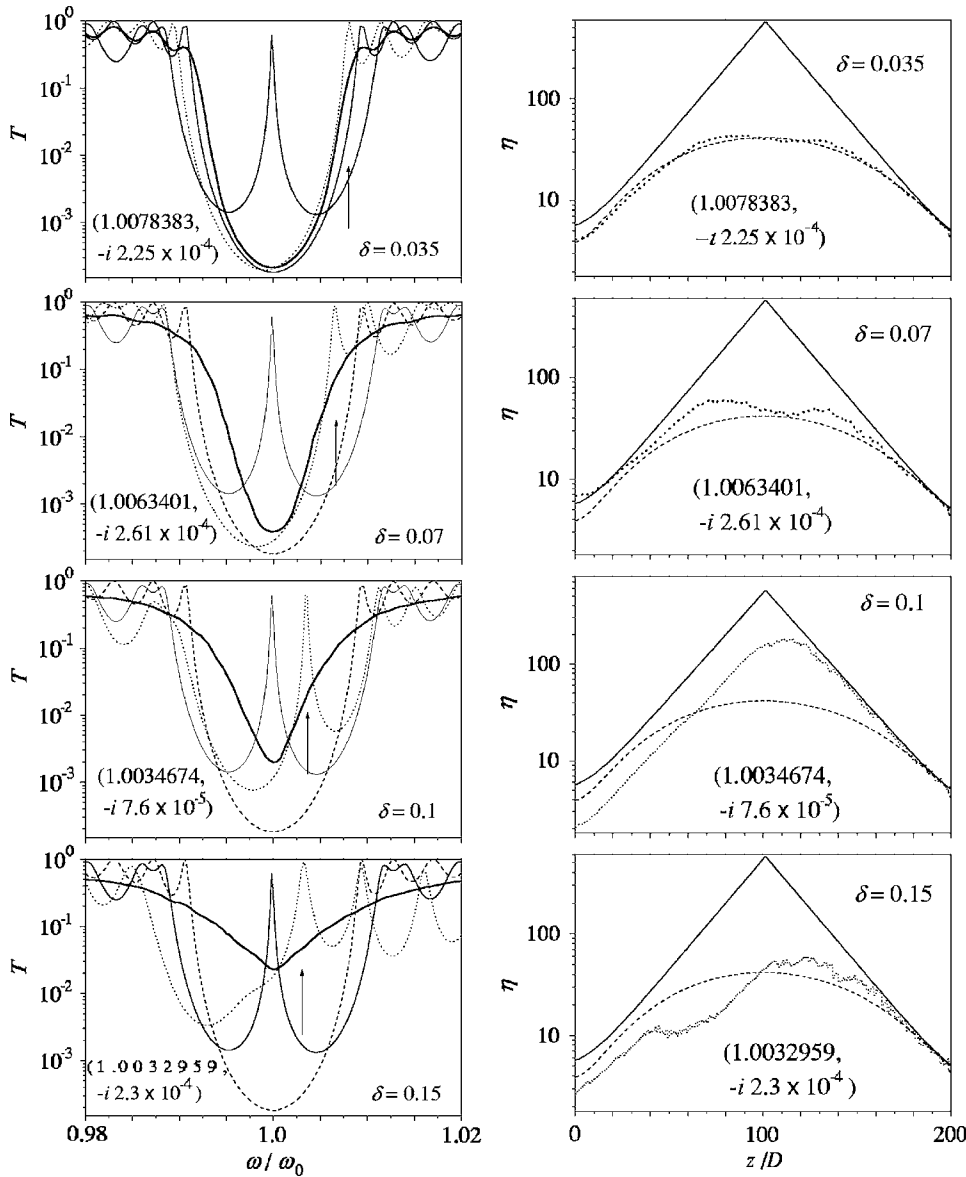


FIG. 3. On the left: transmission spectra for a single structure (dotted line), and averaged over an ensemble of structures (thick solid line). Dashed lines show the spectra for an ideal structure, and the thin solid lines shows the spectra for a microcavity with a half-wavelength core based on an ideal structure. The thickness of the structure is  $L=200D$ , and the modulation of the refractive index is  $g=0.025$ . Arrows point out the frequencies for which the profiles of the density of electromagnetic energy  $\eta$  are shown on the right (dotted lines). For comparison, the profile of an edge state (dashed line) and the microcavity mode (solid line) are also shown.

fies the level of disorder. Disorder can also be introduced by varying the layer thicknesses such that

$$d_{A,B} = d + d\delta P. \quad (9)$$

In both cases the optical lengths  $D_i$  of the unit cells in a particular disordered structure are given by

$$D_i = D(n_A + n_B)/2 = Dn_0(1 + \delta P) = D_0(1 + \delta P), \quad (10)$$

where  $D_0 = n_0 D$  and the range of the random fluctuations in  $D_i/D_0$  is given by  $\delta$ , as shown in Fig. 1(d). An example of the refractive index profile for a disordered structure is shown by the dashed curve in Fig. 1(a). When the refractive indices and thicknesses of the layers are taken to fluctuate simultaneously and independently, and the fluctuation of each quantity is characterized by a top-hat distribution of relative width  $\delta$ , the distribution function of the optical length  $D_i$  of a period of the structure is almost a Gaussian with width close to  $\delta$ , as shown in Fig. 1(d) by the dotted line. We will refer the three models of disorder described

above as “refractive index disorder,” “thickness disorder,” and “Gaussian disorder.”

Figure 2(a) shows the density of modes near the PBG for an ideal structure with  $n_0=2.0$ ,  $g=0.025$ ,  $L=200D$ ,  $\delta=0$  and, on the right, the eigenfrequencies and corresponding lifetimes. In the right-hand diagrams of Fig. 2, the lower horizontal lines show the lifetime of the modes in the structure for which  $g=0$  (i.e., the Fabry-Pérot modes of a uniform structure, with  $\tau\omega_0=580$ ). For the Fabry-Pérot modes of the uniform structure, the inverse lifetime is comparable to the interval between modes, and hence, such states are delocalized according to the Thouless criterion. One can see in Fig. 2(a) that periodic modulation of the refractive index leads to an increase in the lifetime of the eigenmodes, and the increase is more pronounced for the states close to the PBG edges. The states closest to the edge of the PBG are called edge states and were first described in Ref. [17] in the context of distributed feedback lasers. The upper horizontal lines in the right hand diagrams of Fig. 2 ( $\tau\omega_0=4800$ ) show the lifetime of the edge states. According to the Thouless crite-

tion, the edge states in the ideal structure are localized; the inverse lifetime, which is equal to the width of the level  $1/\tau=0.0002\omega_0$ , is more than one order of magnitude less than the interval between the modes. At the same time, the density of electromagnetic energy decays to the edges of the structure more slowly than an exponential.

It is interesting to consider whether there is an upper limit for the lifetime of the modes in such a structure. For an isolated defect (microcavity) in the center of the ideal structure (for example a layer of thickness  $D$  and refractive index  $n_A$ ), the profile of the density of electromagnetic energy of the cavity eigenmodes would decay exponentially, as shown in Fig. 3, and such a mode would possess the maximum lifetime of around  $19\,000/\omega_0$ . In the transmission spectrum of such a structure there is a sharp spike at the center of the PBG, corresponding to the cavity eigenmodes, as shown in Fig. 3.

On the right in Figs. 2(b)–2(e), the solutions of Eq. (7) are plotted as  $(\text{Re}(\omega_i), 1/\text{Im}(\omega_i))$  for  $10^3$  disordered structures with different configurations of the disorder characterized  $\delta=0.035$  (b),  $0.07$  (c),  $0.1$  (d), and  $0.15$  (e). The left-hand side of Figs. 2(b)–2(e) show the density of states averaged over an ensemble of  $10^4$  structures for the three different models of disorder considered. The frequency separation of the levels in the structures is about  $0.004\omega_0$ . Strictly speaking, the density of states diagrams are histograms, but the bin widths are sufficiently small (less than the interval between eigenmodes) so that the histograms are close approximations of the density of states curves. The only exception is the ideal structure, where the density of states is actually a set of Dirac delta functions. The densities of states for “refractive index” and “thickness” disorder with a top-hat distribution of  $D_i$  are practically identical for a given value of  $\delta$ , and very close to the case of “Gaussian” distribution for all values of  $\delta$  considered. Thus we conclude that the density of modes within the PBG of a one-dimensional disordered photonic crystal is defined by the relative fluctuation of the optical length of one period of the structure.

For  $\delta=0.035$  the eigenfrequencies  $\text{Re}(\omega_i)$  and their lifetimes  $\tau_i$  fluctuate near the values corresponding to the eigenmodes of the ideal structure, but the fluctuations of the lifetime of the edge states near the PBG are larger than for those further away. It is apparent in Fig. 3(a) that the profile of the energy density  $\eta$  for a mode of the disordered structure is similar to the profile of the corresponding edge states of the ideal structure. The delta functions in the density of states of the perfect crystal are replaced by Gaussian peaks in Fig. 2(b), and the tails of the peaks penetrate beyond the edges of the PBG. The shape of the tails within the PBG are described to a very high accuracy by the formula

$$\rho \sim \exp\left[-\frac{(\omega - \omega_e)^2}{\Omega^2}\right], \quad (11)$$

where  $\omega_e$  is the angular frequency of the relevant band edge in the crystal and  $\Omega$  is a penetration depth parameter determined by the level of disorder. The tails of the density of modes have the same form at higher levels of disorder, even when the width of the peaks exceeds the separation between

modes. Fits to the numerical results using Eq. (11) are shown in Fig. 2 for the various levels of disorder, along with the values of  $\Omega$  used. The penetration depth  $\Omega$  is found to be linearly proportional to  $\delta$  but does not depend on the length of the structure (as is to be expected since the density of states is a self-averaging quantity). When  $\Omega$  is much less than half the PBG width, the probability of the appearance of modes in the center of the PBG remains virtually negligible.

When  $\delta$  is increased to  $0.07$ , Figs. 2 and 3 show that the edge states penetrate further into the PBG, the fluctuations of the lifetime of the modes increase, and the profile of the states differ markedly from the profiles of the edge states in the ideal structure. The width of the PBG is significantly reduced but nevertheless remains substantial. Eventually, when  $\delta$  is increased to  $0.1$  the probability of the appearance of eigenmodes in any part of the original PBG becomes considerable and the fluctuations in the lifetimes of the eigenstates are greater. For some of the states, the lifetime is comparable to the lifetime of the microcavity mode and the profile of one such mode is shown in Fig. 3. One can see, that the profile of this mode is similar to that of the microcavity mode, in particular there is exponential decay, despite the fact that the fluctuations in refractive index do not appear to provide isolated defects where light can be localized. Nevertheless, at this level of disorder, it is apparent that not only do shifted edge states appear in the PBG, but there are also “states localized in random microcavities” characterized by large lifetimes.

An increase of  $\delta$  to  $0.15$  leads to a decrease in the dip of the density of states, an increase of the fluctuations of the lifetime, and a slight decrease of the mean value of the lifetime. Further increase of  $\delta$  leads to the disappearance of the effects associated with the periodic modulation of the refractive index, and the system becomes completely disordered. In this regime the values of the lifetimes suggest that the majority (but not all) of these states are localized.

In the transmission spectra of Fig. 3, the eigenstates manifest themselves as spikes in the region of the PBG, and the greater the lifetime, the sharper the spikes. In the PBG region there is a dip in the transmission spectra averaged over an ensemble of the structures, but with increasing  $\delta$  the dip becomes shallower, and its shape varies.

By modeling structures with different values of relative band width  $\Delta\omega/\omega_0$  ranged in the interval from  $0.004$  to  $0.16$  (which corresponds to high refractive index contrast structure of experimental interest), we have found that the penetration depth  $\Omega$  is proportional to the square root of the relative gap width. However,  $\Omega$  is actually a function of the three independent parameters  $\Delta\omega$ ,  $\omega_0$ , and  $\delta$ . In Fig. 4 the dimensionless quantity  $(\Omega/\delta\omega_0)\sqrt{\omega_0/\Delta\omega}$  is plotted as a function of the average refractive index in the structure  $n_0$ , which is related to the frequency of the center of the PBG by the formula  $\omega_0 = \pi c/(n_0 D)$ . The plot leads us to conclude that the penetration depth is described by the formula

$$\frac{\Omega}{\omega_0} \approx \frac{\delta}{5} \sqrt{\frac{\Delta\omega}{\omega_0}}, \quad (12)$$

i.e., the relative penetration depth exhibits a universal dependence on the relative gap width.

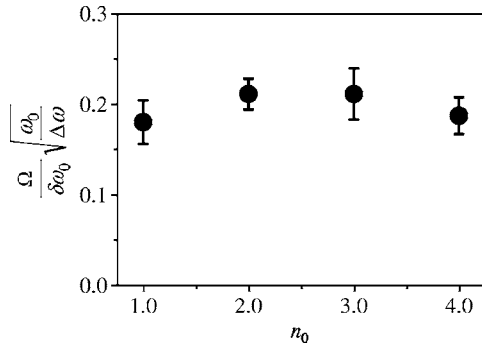


FIG. 4. The quantity  $(\Omega/\delta\omega_0)\sqrt{\omega_0/\Delta\omega}$  for structures characterized by different values of the average refractive index  $n_0$ . The vertical bars indicate the standard deviation of this quantity.  $10^4$  structures were modeled for each set of the parameters  $n_0$ ,  $g$ , and  $\delta$ . The values of the relative gap width  $\Delta\omega/\omega_0$  in the structures considered ranged from 0.004 to 0.16.

Equation (12) provides a means to specify a practical criterion for the resilience of the PBG to the presence of the disorder. Assuming that for a particular application there is a certain acceptable level of the density of states at the center of a band gap described by a suppression factor  $S_{th}$ , which is defined as the ratio of the densities of states at the center and the edge of PBG, the threshold value of the disorder parameter  $\delta_{th}$  is

$$\delta_{th} = \frac{5}{2\sqrt{-\ln S_{th}}} \sqrt{\frac{\Delta\omega}{\omega_0}}. \quad (13)$$

For example, suppression of the density of states at the center of PBG by a factor  $10^{-8}$ , would corresponds to  $4.5\Omega \approx \Delta\omega/2$ , and a threshold disorder parameter given by  $\delta_{th} \approx \sqrt{(\Delta\omega/\omega_0)/3}$ . Note that the square root of the logarithm in Eq. (13) varies very slowly with the change of the argu-

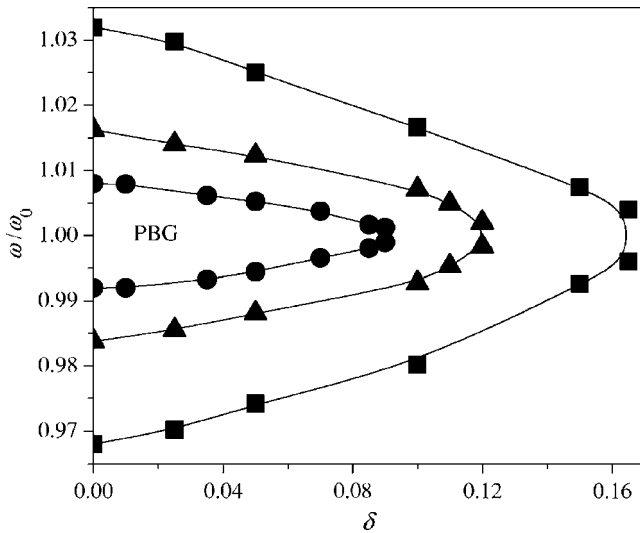


FIG. 5. (a) Boundary of the PBG as a function of disorder parameter  $\delta$  for structures with  $n_0=2.0$  and different modulations of the refractive index  $g$ : circles  $g=0.025$ , triangles  $g=0.05$ , and squares  $g=0.1$ .

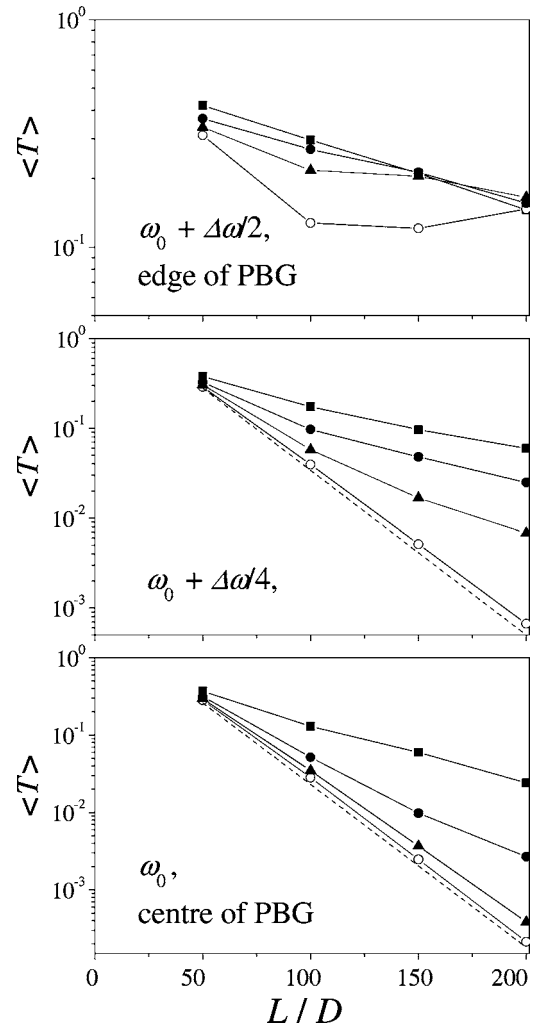


FIG. 6. Transmission coefficient averaged over an ensemble of structures at frequency  $\omega_0$  (center of PBG), at frequency  $\omega_0 + \Delta\omega/4$ , and at frequency  $\omega_0 + \Delta\omega/2$  (edge of PBG) as a function of the thickness of the structure  $L$ , for different values of  $\delta=0.035$  (open circles),  $\delta=0.07$  (triangles),  $\delta=0.1$  (solid circles), and  $\delta=0.15$  (squares). For comparison, the corresponding dependences for an ideal structure are shown by the dashed lines. The mean and modulation of the refractive index are  $n_0=2.0$  and  $g=0.025$ .

ment, and the above estimate can be considered as an almost universal criterion for the stability of the PBG in one-dimensional photonic crystals in the presence of disorder.

Figure 5 shows how the frequencies of the edges of the PBG (determined by the penetration depth  $\Omega$ ) vary with the value of the disorder parameter  $\delta$ , for structures with different levels of modulation of the refractive index ( $g=0.025$ ,  $g=0.05$ , and  $g=0.1$ ). It can be seen, that when the disorder is small, the gradient of the PBG boundary curves  $\omega(\delta)$  are small (possibly equal to zero, but numerical modeling does not allow us to show that conclusively). This behavior means that even for a small modulation of the refractive index the PBG is resilient to the disorder, which is contrary to the accepted view that the PBG is filled with localized photonic states even with weak disorder [3,6]. The tops of the curves correspond to the threshold values of the disorder parameter  $\delta_{th}$ , and it is apparent that an increase of the modulation of



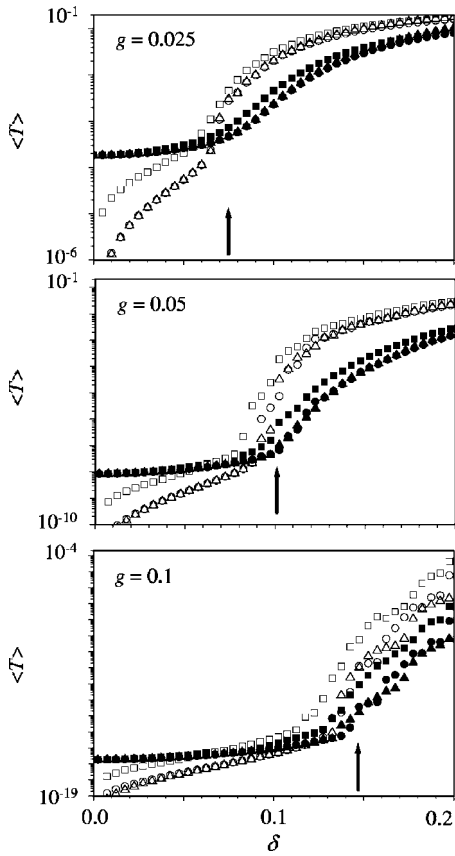


FIG. 7. Transmission coefficient averaged over  $10^6$  structures (solid symbols) and its standard deviation (open symbols) as a function of the disorder parameter  $\delta$  for the photonic crystals with  $n_0=2.0$  and different levels of modulation of the refractive index:  $g=0.025$ ;  $0.05$ ; and  $0.1$ . Circles and triangles corresponds to the refractive index and thickness disorder with top-hat distribution of  $D_i$ ; squares corresponds to the Gaussian distribution. Vertical arrows indicate the threshold levels of disorder predicted by the formula  $\delta_{th} = \sqrt{(\Delta\omega/\omega_0)}/3$ .

the refractive index  $g$  leads to an increase of  $\delta_{th}$  as described by Eq. (13).

The dependence on sample thickness  $L$  of the transmission coefficient averaged over an ensemble of structures, is shown in Fig. 6. Within the PBG the ensemble-averaged transmission coefficient  $\langle T \rangle$  decays exponentially with increasing sample thickness  $L$

$$\langle T \rangle = \exp(-L/\xi), \quad (14)$$

where the attenuation length  $\xi$  increases with  $\delta$ . At the edge of the PBG,  $\langle T \rangle$  demonstrates more complicated behavior when  $\delta$  is small; in this case  $\langle T \rangle$  is determined by the frequency of an edge state, which depends on the thickness of sample  $L$ , but when  $\delta$  is large enough  $\langle T \rangle$  decays exponentially with increasing  $L$ .

The existence of a threshold level of disorder is illustrated in Fig. 7, where the dependences on the disorder parameter  $\delta$  of the transmission coefficient  $\langle T \rangle$  and its standard deviation at the center of the band gap for structures, characterized by different refractive index modulation  $g$  are shown for the

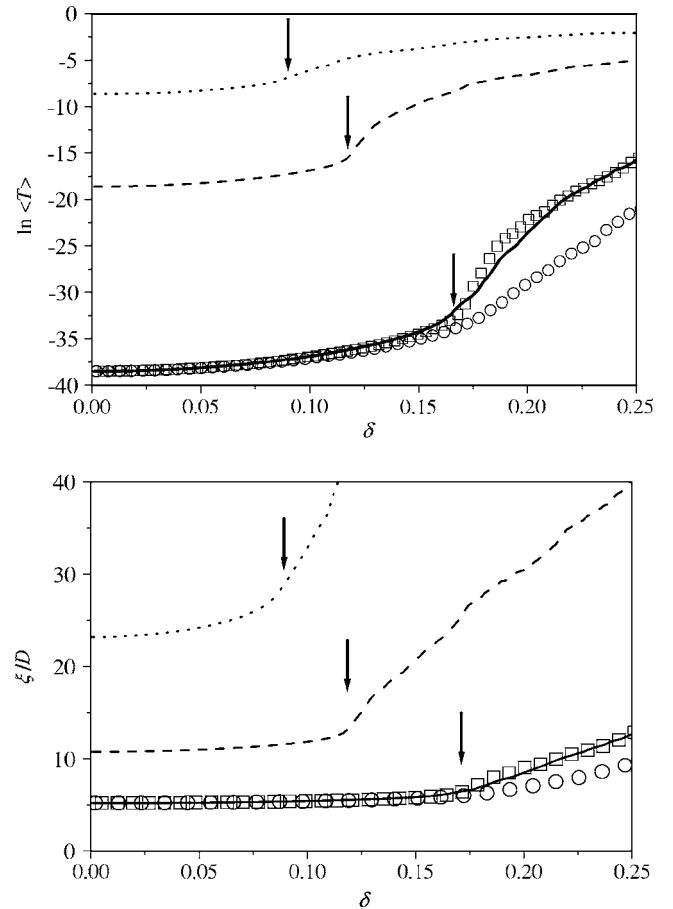


FIG. 8. Dependence on the disorder parameter  $\delta$  of the transmission coefficient at the center of the PBG, averaged over an ensemble of the structures, its logarithm and the attenuation length  $\xi$  for the structures with modulation of the refractive index given by  $g=0.025$  (dotted line),  $g=0.05$  (dashed line),  $g=0.1$  (solid line). Symbols show the dependences obtained for the case  $g=0.1$  of by the transformation  $(\ln\langle T \rangle \rightarrow \alpha \ln\langle T \rangle, \delta \rightarrow \delta\sqrt{\alpha})$  or  $(\xi \rightarrow \xi/\alpha, \delta \rightarrow \delta\sqrt{\alpha})$  of the results for the structures with  $g=0.025$  (circles) and  $g=0.05$  (squares). Here  $\alpha$  is the ratio of the attenuation lengths for the structure with either  $g=0.025$  or  $g=0.05$  and the attenuation length for the structure with  $g=0.1$ . Arrows indicate the threshold values of  $\delta$ . The thickness of the structure is  $L=200D$ .

three models of disorder. For all the cases considered the dependences are characterized by a threshold; when  $\delta < \delta_{th}$ ,  $\langle T \rangle$  grows slowly with increasing  $\delta$ , and the attenuation length  $\xi$  virtually does not change. When  $\delta$  reaches  $\delta_{th}$ ,  $\langle T \rangle$  grows much faster with increasing  $\delta$ . The threshold in the dependence of  $\langle T \rangle$  on  $\delta$  is accompanied by a crossing of  $\langle T \rangle$  and its standard deviation; below threshold  $\langle T \rangle$  is larger than its standard deviation, but smaller for  $\delta > \delta_{th}$ . For all cases the position of threshold is well described by the formula  $\delta_{th} \approx \sqrt{(\Delta\omega/\omega_0)}/3$ .

Such behavior can be easily explained. The increase of  $\langle T \rangle$  is a consequence of the appearance of sharp spikes, corresponding to localized eigenmodes, in the transmission spectrum of individual structures, as shown in Fig. 3. When  $\delta < \delta_{th}$ , the increase of the transmission coefficient is provided by the tails of such spikes and therefore is very small.

When  $\delta > \delta_{th}$ , localized states and corresponding peaks in the transmission spectra can appear in the center of the PBG, and  $\langle T \rangle$  starts to grow faster with increasing  $\delta$ . Note, that for an individual structure in the ensemble, when  $\delta > \delta_{th}$  the transmission coefficient at a given frequency can be any value from zero to one, and the standard deviation of  $\langle T \rangle$  exceeds its mean value.

For the refractive index and thickness disorder, the dependences of  $\langle T \rangle$  and its standard deviation on  $\delta$  are identical, but for the Gaussian distribution the threshold is achieved at a slightly smaller value of  $\delta$ . This is further confirmation that the relative fluctuation of the optical length of the unit cell is an appropriate parameter to describe the disorder.

Figure 8 shows the dependence on  $\delta$  of  $\ln \langle T \rangle$  and the attenuation length  $\xi = -L / \ln \langle T \rangle$  at the center of the PBG, for structures with  $g=0.025$ ,  $g=0.05$ , and  $g=0.1$ . The dependence of  $\delta_{th}$  on the relative width of the PBG (or on the attenuation length  $\xi_0$ ) in Eq. (13) has an interesting consequence. If  $\alpha$  is the ratio of the attenuation lengths  $\xi_0^{(1)}$  and  $\xi_0^{(2)}$  for two ideal structures with different modulations of the refractive indices  $g^{(1)}$  and  $g^{(2)}$ , then

$$\alpha = \frac{\xi_0^{(2)}}{\xi_0^{(1)}} = \frac{g^{(1)}}{g^{(2)}} = \left( \frac{\delta_{th}^{(1)}}{\delta_{th}^{(2)}} \right)^2. \quad (15)$$

As a result, it turns out that the dependences of the transmission coefficient  $\langle T \rangle$  (or attenuation length  $\xi$ ) on  $\delta$  for the two structures are coupled remarkably well by the relations

$$\ln \langle T^{(2)}(\delta) \rangle = \alpha \ln \langle T^{(1)}(\delta \sqrt{\alpha}) \rangle \quad (16)$$

or

$$\alpha \xi^{(2)}(\delta) = \xi^{(1)}(\delta \sqrt{\alpha}). \quad (17)$$

In Fig. 7 the squares show the result of the transformations (16) and (17) on  $\langle T \rangle(\delta)$  or  $\xi(\delta)$  for the structure with  $g=0.05$ , when  $\alpha = \xi_0(g=0.05) / \xi_0(g=0.1)$ . The circles show the result of the corresponding transformation for the structure with  $g=0.025$ , and  $\alpha = \xi_0(g=0.025) / \xi_0(g=0.1)$ . For the structures with  $g=0.05$  and  $g=0.1$  the transformations (16) and (17) couple the dependences  $\langle T \rangle(\delta)$  or  $\xi(\delta)$  with very high accuracy. For the structure with  $g=0.025$ , when  $\delta$  is larger than the threshold value, some deviation occurs at the higher values of  $\delta$  due to the fact that the attenuation length is comparable to the sample size, and the influence of the boundaries is substantial.

The transformation in Eq. (16) or Eq. (17), reflects a universal behavior of the transmission coefficient (and attenuation length) in disordered photonic crystals and could be useful in the development of analytical theories of such systems.

### III. CONCLUSIONS

For the one-dimensional photonic crystals of finite size considered, the states closest to the band gap have frequencies and lifetimes which are defined by the periodic dielectric structure and its length. The introduction of a small level of disorder results in small perturbations of the frequencies and lifetimes of those states which depend on the particular configuration of the disorder. As the disorder is increased, the fluctuations of the frequencies in an ensemble of systems increases and eventually it is no longer possible to associate a particular state with a counterpart in the crystalline system.

The tail of the density of states in the band gap is characterized by a certain penetration depth. As a result, there is a threshold level of disorder, below which the probability of the appearance of photonic eigenstates at the center of photonic band gap essentially vanishes. The relation between the relative penetration depth, relative gap width, and the parameter defining the level of disorder has been found.

The transmission spectrum of any individual disordered sample has a spiky appearance with substantial transmission at frequencies corresponding to states induced into band gap by the disorder. However, the attenuation length of the ensemble-averaged transmission of radiation at the gap-center frequency does not grow significantly with increasing disorder, and the standard deviation of the transmission is smaller than its mean value until the threshold value of disorder is reached. Beyond the threshold there is a fast growth of the attenuation length with increasing disorder reflecting the increasing probability of a state being found at the gap center, and the standard deviation of the transmission exceeds its mean value.

Finally, the results demonstrate how a simple formula relates the logarithm of the transmission to the level of periodic refractive index modulation and the disorder.

### ACKNOWLEDGMENTS

The work was supported by an EPSRC grant. The authors are grateful to Professor Yu Rubo and Professor S. G. Tikhodeev for fruitful discussions.

- 
- [1] J. D. Joannopoulos, R. D. Meade, and J. N. Winn, *Photonic Crystals: Molding the Flow of Light* (Princeton University Press, Princeton, NJ, 1995).
  - [2] K. Sakoda, *Optical Properties of Photonic Crystals* (Springer, Berlin, 2001).
  - [3] S. John, Phys. Rev. Lett. **58**, 2486 (1987).
  - [4] P. W. Anderson, Phys. Rev. **109**, 1492 (1958).
  - [5] N. F. Mott, *Metal-Insulator Transitions* (Taylor & Francis,

London, 1974).

- [6] *Photonic Band Gap and Localization*, NATO ASI Series B No. 308, edited by C. M. Soukoulis (Plenum, New York, 1993).
- [7] E. Abrahams, P. W. Anderson, D. C. Licciardello, and T. V. Ramakrishnan, Phys. Rev. Lett. **42**, 673 (1979).
- [8] P. W. Anderson, D. J. Thouless, E. Abrahams, and D. S. Fisher, Phys. Rev. B **22**, 3519 (1979).
- [9] M. P. Van Albada and A. Lagendijk, Phys. Rev. Lett. **55**, 2692

- (1985).
- [10] P. E. Wolf and G. Maret, Phys. Rev. Lett. **55**, 2696 (1985).
  - [11] Y. Kuga and A. Ishimaru, J. Opt. Soc. Am. A **1**, 831 (1984).
  - [12] A. P. Vinogradov and A. M. Merzlikin, Phys. Rev. E **70**, 026610 (2004).
  - [13] *Confined Electron and Photon, New Physics and Applications*, NATO ASI Series No. 340, edited by E. Burstein and C. Weisbush (Plenum, New York, 1995).
  - [14] *Photonic Band Gap Materials*, NATO ASI Series E Applied Sciences No. 315, edited by C. M. Soukoulis (Kluwer, Dordrecht, 1996).
  - [15] L. I. Deych, D. Zaslavsky, and A. A. Lisyansky, Phys. Rev. Lett. **81**, 5390 (1998).
  - [16] L. I. Deych, A. A. Lisyansky, and B. L. Altshuler, Phys. Rev. Lett. **84**, 2678 (2000).
  - [17] H. Kogelnick and C. V. Shank, J. Appl. Phys. **43**, 2327 (1972), the coupled wave theory developed in this paper is a rather rough approximation (the authors neglect the second derivative of the amplitude of the waves on the spatial coordinate) and therefore it cannot be applied to the analysis of disordered systems.
  - [18] V. A. Kosobukin, Sov. Phys. Solid State **32**, 227 (1990).
  - [19] T. F. Krauss, R. M. D. L. Rue, and S. Brand, Nature (London) **383**, 699 (1996).
  - [20] Y. A. Vlasov, V. N. Astratov, O. Z. Karimov, A. A. Kaplyanskii, V. N. Bogomolov, and A. V. Prokofiev, Phys. Rev. B **55**, R13357 (1997).
  - [21] A. V. Baryshev, A. V. Ankudinov, A. A. Kaplyanskii, V. A. Kosobukin, M. Limonov, K. B. Samusev, and D. E. Usvyat, Phys. Solid State **44**, 1648 (2002).
  - [22] M. Muller, R. Zentel, T. Maka, S. G. Romanov, and C. M. S. Torres, Adv. Mater. (Weinheim, Ger.) **12**, 1499 (2000).
  - [23] D. Norris and Y. Vlasov, Adv. Mater. (Weinheim, Ger.) **13**, 371 (2001).
  - [24] Y. A. Vlasov, M. A. Kaliteevski, and V. V. Nikolaev, Phys. Rev. B **60**, 1555 (1999).
  - [25] M. A. Kaliteevski, J. M. Martinez, D. Cassagne, and J. P. Albert, Phys. Rev. B **66**, 113101 (2002).
  - [26] M. A. Kaliteevski, J. M. Martinez, D. Cassagne, and J. P. Albert, Phys. Status Solidi A **195**, 612 (2003).